



## **Preparation, Optimization and Characterization of Recombinant Typhoid (Ty21a) Antigen Encapsulated Eudragit Coated Dextran Nanoparticles**

**Ramakant Prajapati\*, Vishal Bharat Babar**

School of pharmacy, SunRise University, Alwar, Rajasthan 301028, India

E-mail ID: [mr.ramakant1981@rediffmail.com](mailto:mr.ramakant1981@rediffmail.com)

### **ABSTRACT**

*The development of effective vaccines against Typhoid fever remains a global health priority, especially in regions with a high burden of the disease. In this study, we worked on the preparation, optimization, and characterization of recombinant Typhoid (Ty21a) antigen-encapsulated Eudragit-coated dextran nanoparticles. These nanoparticles serve as a novel platform for the delivery of the Ty21a antigen, offering potential improvements in vaccine stability and efficacy. The synthesis process was systematically optimized to achieve ideal nanoparticle size, morphology, and surface properties using various formulation parameters. Physicochemical characterization confirmed the production of well-defined nanoparticles with efficient Ty21a antigen encapsulation. In vitro release studies revealed sustained and controlled antigen release from the Eudragit-coated nanoparticles, indicative of their potential for providing long-lasting immune stimulation. This research signifies the potential of recombinant Typhoid antigen-encapsulated Eudragit-coated dextran nanoparticles as a promising platform for next-generation vaccines, offering enhanced immunogenicity and controlled antigen delivery, with substantial implications for global health initiatives targeting Typhoid fever.*

**Keywords:** Antigen, Controlled release, Immunogenicity, Optimization. Nanoparticles, Vaccine.

Received 23.09.2023

Revised 07.10.2023

Accepted 21.10.2023

### **INTRODUCTION**

Vaccines have played a vital role in preventing infectious diseases, with three main categories in use for human immunization: live-attenuated, inactivated, and subunit vaccines. However, the evolution of gene therapy technologies has ushered in a new era in vaccinology, exemplified by the recent development of mRNA vaccines, such as those for COVID-19. Live-attenuated vaccines contain weakened forms of pathogens, either viral or bacterial, capable of replication within a host to initiate an immune response. Notable examples include the MMR (Measles, Mumps, and Rubella), chickenpox, rotavirus, seasonal influenza, and oral polio vaccines [1]. In contrast, inactivated vaccines, like inactivated polio and hepatitis A vaccines, involve pathogens rendered noninfectious to stimulate immunity. While both vaccine types have demonstrated clinical safety and have been in use for decades, they exhibit limitations such as the need for multiple doses, suboptimal immunity, less-than-desirable immunogenicity, potential inflammation, uncontrolled replication, and the risk of reversion to a pathogenic state for attenuated vaccines [2].

Subunit vaccines consist of non-living antigens, including specific antigen proteins or epitopes capable of recognizing and binding to antibodies or T-cells. These vaccines offer several advantages, such as cost-effectiveness, stability, and safety, resulting in lower immunogenicity and fewer adverse reactions when compared to live-attenuated and inactivated vaccines. Examples of subunit vaccines include the hepatitis B and pertussis vaccines. Subunit vaccines can be further categorized into protein-based, polysaccharides, conjugates, and toxoids [3].

In the protein-based category, a specific protein from the antigen is used to stimulate an immune response. Polysaccharide subunit vaccines mimic the polysaccharide capsules of infectious bacteria, triggering an immune response [4]. However, both protein-based and polysaccharide subunit vaccines are susceptible to denaturation and degradation due to changes in pH or the presence of proteolytic enzymes. Conjugate subunit vaccines can evoke responses similar to polysaccharide subunit vaccines but often include a carrier protein to extend protective immunity. Notable examples include the diphtheria and tetanus vaccines. Toxoid vaccines consist of inactivated bacterial toxins and are considered safe and stable against

pathogens, as seen in the diphtheria and tetanus vaccines [5]. It is important to note that subunit vaccines generally exhibit weaker immunogenicity compared to live-attenuated vaccines. In the present study we have worked on the preparation, optimization and characterization of recombinant typhoid (Ty21a) antigen encapsulated eudragit coated dextran nanoparticles [6].

**MATERIAL AND METHODS**

Dextran, and Eudragit S100 were purchased from SD fine chemicals, Mumbai. Typhoid (Ty21a) antigen was procured from Merck, Mumbai. Bovine Serum Albumin was purchased from Qualigens Pharma Private Limited, Mumbai. Dialysis membrane were procured from Himedia (Mumbai, India). All the other chemicals used were of analytical grade. Double distilled water (DDW) was used throughout the study wherever needed.

**Identification of Antigen for Protein using Bradford reagent by UV Spectroscopic Method**

In the present study Bovine Serum Albumin (BSA) was used as model antigen and Recombinant Typhoid (Ty21a) Antigen was used as candidate antigen. BSA is a useful antigen because of its low cost, high purity and ready availability for investigation of immunogenic properties of carrier associated, covalently linked or the entrapped macromolecular antigen within the carrier. Since Typhoid (Ty21a) Ag is very expensive molecule, it was thought worthwhile to use it after optimization and characterization of the formulation. Absorbance spectra of the Bradford reagent and the Bradford reagent bound to 20µg of BSA standard. The free reagent has an absorbance peak of 595nm (Figure 1). The unbound dye partially overlaps with the bound form of the reagent and thus leads to the nonlinear response of the Bradford assay [7].

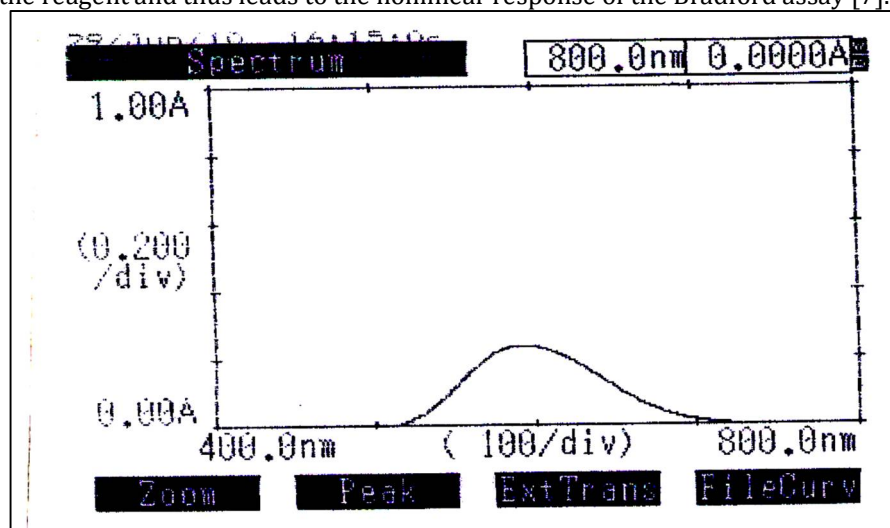
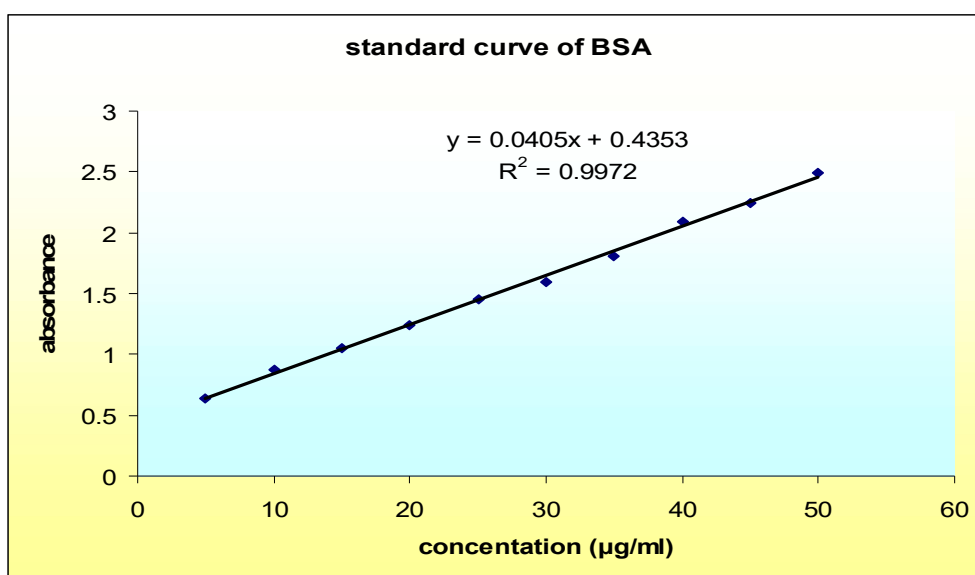


Figure 1: Absorbance Spectra of Bradford Reagent Complex with protein (Absorbance Peak at 595 nm)

Table 1: Preparation of standard curve of BSA using Bradford protein Estimation method

S.No.	Concentration (µg/ml)	Absorbance	Regressed Absorbance	Statistical Parameters
1.	10	0.632	0.6378	Equation of line Y = 0.0405x + 0.4353 R <sup>2</sup> = 0.9972
2.	20	0.869	0.8403	
3.	30	1.054	1.0428	
4.	40	1.246	1.2453	
5.	50	1.455	1.4478	
6.	60	1.592	1.6503	
7.	70	1.803	1.8528	
8.	80	2.093	2.0553	
9.	90	2.247	2.2578	
10.	100	2.492	2.4603	



**Figure 2: Standard curve of BSA by using Bradford reagent at  $\lambda_{\max}$  595nm.**

#### **Formulation of Dextran nanoparticles**

The dextran-based nanoparticles were prepared by the process as follows: 5.0 mg dextran was dissolved in 50 ml deionised water at 25°C under gentle stirring and nitrogen bubbling, then the solution of a designated amount of CAN (cerium ammonium nitrate) in 1.25 ml 0.1 N nitric acid and a designated amount of AA (Acrylic acid) were successively added. Twenty minutes later, MBA (N, N-Methylene bisacrylamide) was added and the reaction was kept at 30°C for 4 h. Thereafter, 1 M NaOH was added to neutralize the reaction system [8].

Finally, the reaction solution was dialyzed against deionised water for 3 days using the membrane bag with a 14,000 cut-off molecular weight (MWCO) to remove the un-reacted monomers and the un-grafted PAA. One ml (1mg/ml) of BSA Solution for loading on dextran nanoparticles was added and stirred at 900 rpm for 4hrs. The final aqueous solution was lyophilized to get solid nanoparticles and same procedure was followed for the preparation of typhoid antigen loaded dextran nanoparticles. For investigating the influence of the ratio of reagents on the resultant nanoparticles, several kinds of nanoparticles were developed under different ratios of reagents. In order to explore the mechanism of this one-step synthesis and investigate the importance of the complexation of AA and dextran during synthesis, N-isopropylacrylamide (NIPAM) was chosen as a substitute of AA in the synthesis of dextran based nanoparticles. NIPAM is also a monomer but has not complexation with dextran.

#### **Eudragit coating on dextran nanoparticles**

The coating dispersion consisted of 2 % of coating material (Eudragit S 100) were dissolved in organic solvent ratio (2:1) acetone: ethanol. A polymer solution was prepared by dissolving 0.8 g of Eudragit solution in 100 ml of acetone and ethanol (ratio 2:1). Dextran nanoparticles (0.8 g) was suspended in the polymer solution using ultra sonicator (40 KHz) to break up any agglomerates in the polymer and nanoparticles suspension [9].

The enteric coating on the nanoparticles bearing BSA and Ty Ag was performed by using Supercritical Anti solvent process. The enteric coating solution was prepared as reported by The enteric coating solution was prepared by first making milky latex of Eudragit-S 100 using organic solvent (acetone: ethanol, ratio 2:1). After 1 hour Triethylamine citrate (60%) was added and stirred was continued for 30 min. Talc was added to the milky latex as an antitacking agent. Throughout the coating process the coating dispersion was stirred using a magnetic stirrer. Then the nanoparticles were dipped in coating solution then filtered and dried the coated formulation [10].

#### **Optimization of formulation**

##### **Process variable on the basis of particle size and entrapment efficiency**

Different formulations of nanoparticles were prepared using different concentration of Acrylic acid (AA) e.g., 0.1, 0.3, 0.5, 0.7 and 0.9. Formulations were characterized by transmission electron microscopy (TEM) for shape and size. At concentration 0.5% w/v AA, particles were having size about  $192 \pm 34$  nm. and entrapment efficiency was found to be  $68 \pm 2.7$  % [11].

**Table 2: Effect of AA concentration on the particle size**

FORMULATION CODE	A1	A2	A3	A4	A5
DEXTRAN: AA (w/v)	5:0.1	5:0.3	<b>5:0.5</b>	5:0.7	5:0.9
PARTICLE SIZE (nm)	486±25	266±25	<b>192±34</b>	280±30	370±30
% ENTRAPMENT	54±2.3	61±1.6	<b>68±2.7</b>	71±3.1	62±2.4

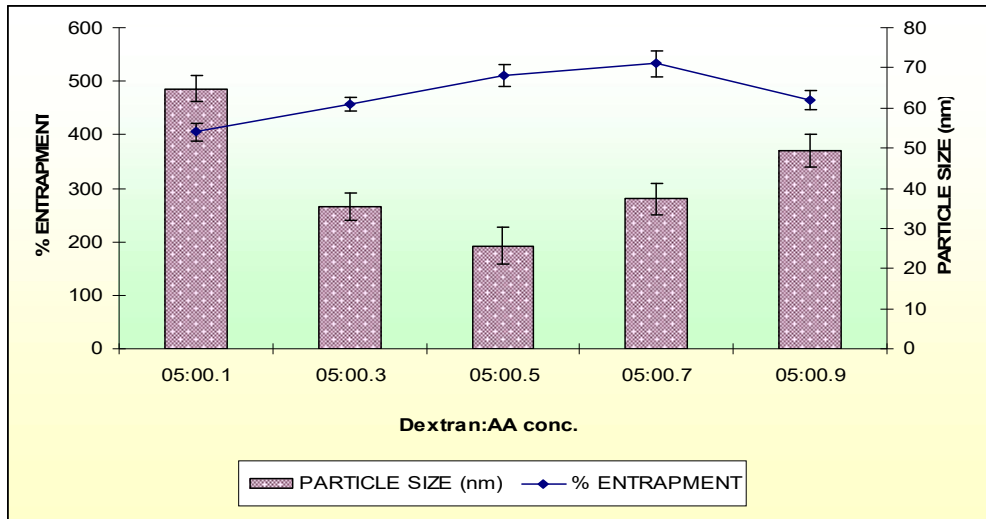


**Figure 3: Optimization of AA Concentration**

Different stirring time was used to optimize nanoparticles size and entrapment efficiency. Different formulations were developed by stirring for 30, 60, 90, 120 and 150 min. and characterized for size and entrapment efficiency [12].

**Table 3: Effect of stirring time on the particle size**

FORMULATION CODE	A3a	A3b	A3c	A3d	A3e
STIRRING TIME (min)	30	60	90	<b>120</b>	150
PARTICLE SIZE (nm)	780±30	470±30	380±30	<b>192±33</b>	281±30
% ENTRAPMENT	28±1.7	48±3.2	61±3.3	<b>68± 2.2</b>	69±3.4

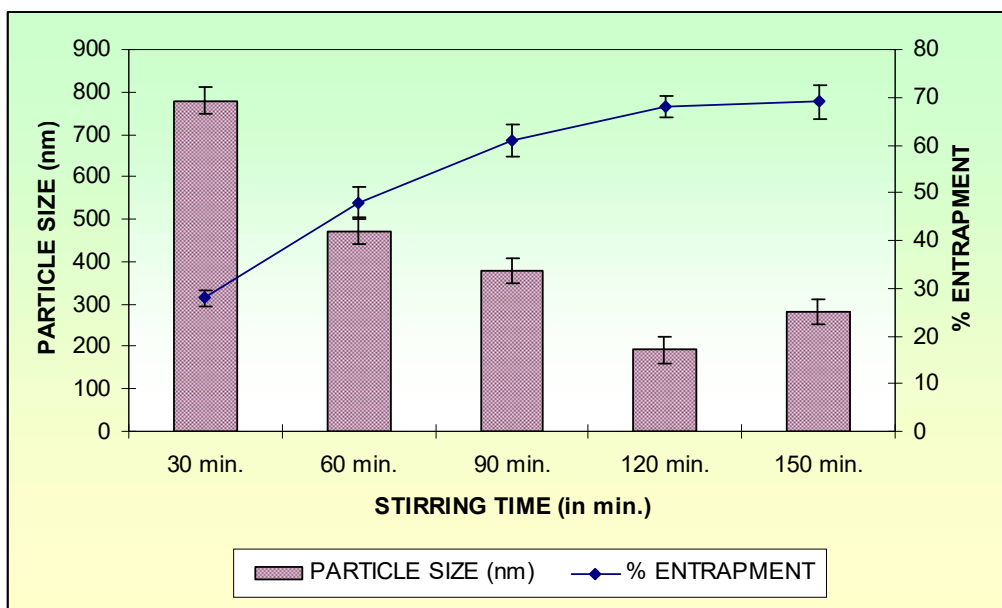


**Figure 4: Optimization of Stirring Time**

### Optimization of Coating Materials

The core: coat ratio was optimized in terms of particle size. The core: coat ratio was varied from 1: 5 to 1: 25. The results are given in table 4 and graphically presented in Figure 5.

**Table 4: Effect of core: coat ratio on particle size and shape on Eudragit coated dextran nanoparticles**

S.No.	Formulation Code	Core:coat ratio	Particle size (nm)	% Entrapment
1	A3d <sub>4</sub> 1	(1: 5)	284±40	65±2.3
2	A3d <sub>4</sub> 2	(1:10)	304±46	67±1.9
3	A3d <sub>4</sub> 3	(1:15)	324±52	69±1.5
4	A3d <sub>4</sub> 4	(1:20)	344±58	71±1.1
5	A3d <sub>4</sub> 4	(1:25)	364±64	73±0.7

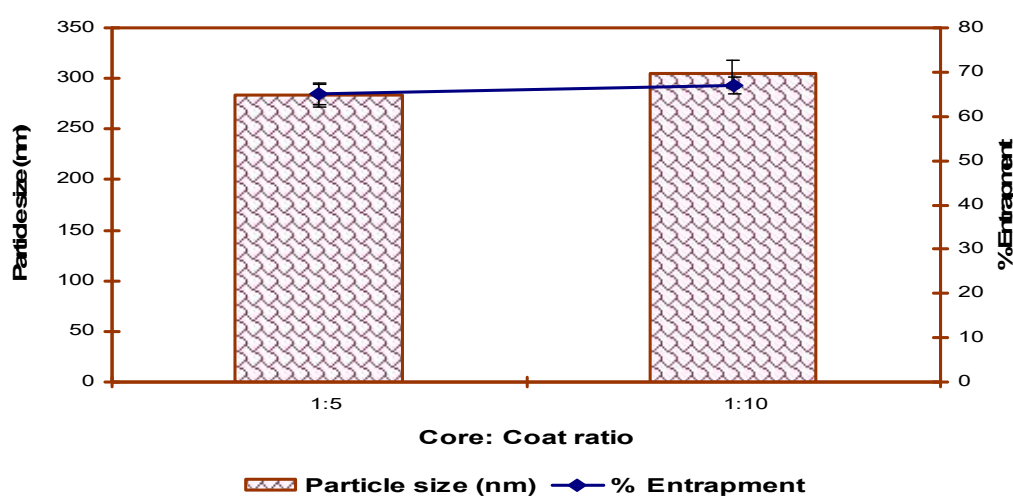


**Figure 5: Optimization of Core: Coat Ratio**

### Final Optimized Formulas

The final formula obtained after optimizing AA concentrations, core: coat ratio, stirring time and stirring speed (Table 5).

**Table 5: Final optimized formula of Eudragit coated dextran nanoparticles**

FORMULATION CODE	AA CONC.	Coat:coat ratio	STIRRING TIME	STIRRING SPEED	PARTICLE SIZE	% Entrapment
A3d <sub>4</sub> 1	0.5	(1: 5)	120 min.	1600 rpm	203±33 nm.	71±1.7

### Characterization of Nanoparticles

#### Transmission Electron microscopy (TEM)

TEM was performed with an accelerating voltage of 100 kV. A drop of the sample was placed on a carbon coated copper grid to leave a thin film on the grid. The film was negatively stained with 15 phosphotungstic acid. A drop of the staining solution was added on the film and the excess of the solution was drained of with a filter paper. The grid was allowed to air dry thoroughly and samples were viewed on TEM [13].

#### Zeta (ζ) potential

The zeta potential of the polymer and nanoparticles was deduced from the electrophoretic mobility of the particles by Doppler Electrophoresis (Zetasizer Nano serie. Malvern Instrument Ltd., Worcestershire, UK) in HEPES buffer pH 7.4 after suitable dilution (1/ 200 (v/v)) of the different nanoparticles suspension [14].

#### Size measurement

The hydrodynamic mean diameter and the size distribution of the nanoparticles were determined at 25 °C by quasielastic light scattering using a Zeta Nanosizer (Malvern instrument, UK). The scattered angle was fixed at 90°. The derived count rate (kcps) was 38128.5250 [14].

#### Loading Efficiency of BSA Loaded Nanoparticles

The amount of protein entrapped in the nanoparticles was calculated from the difference between the total amount added to the loading solution and the amount of non-entrapped protein remaining in the



supernatant. BSA concentrations in the supernatant were measured by the Bradford protein assay method. Aliquot of the resulting nanoparticles suspension was then separated by centrifugation for 20 min. The supernatant was then separated from the nanoparticles. The amount of non-entrapped protein remaining in the supernatant was measured by the Bradford protein assay method. A non-loaded nanoparticles suspension was used as a blank [15].

#### **In Vitro Release Studies**

Nanoparticles equivalent to 10 mg of drug from each batch were taken into a 250 ml conical flask and 100 ml of pH 1.2 and pH 7.4 phosphate buffer saline was added to it, then the flask was kept in a metabolic shaker and the shaker was adjusted to 80 horizontal shakes per minute at  $37^{\circ}\text{C} \pm 0.5^{\circ}\text{C}$ . Ten ml of the medium was withdrawn at various time intervals of 1, 2, 4, 8, 16, 24 hrs and replaced by the same volume of phosphate buffer saline. The samples were diluted suitably with methanolic PBS and the drug released was estimated in each batch by UV spectrophotometer at 595 nm [16].

### **RESULTS AND DISCUSSION**

The dextran nanoparticles were successfully prepared by one step synthesis and ion-cross linking method using AA as a cross linker. Formula for Nanoparticles preparation was obtained after optimizing the particle size and entrapment efficiency by AA concentration, Stirring time, Stirring speed. The aim of optimization was to prepare polymer nanoparticles with a particle size suitable for uptake by antigen presenting cells and the cells of Gut-associated lymphoid tissue (GALT) along with spherical shape and the highest antigen loading.

The process variables (amount of dextran, stirring time and % AA) were optimized with respect to mean particle size, shape and % entrapment efficiency. The size of nanoparticles decreased slightly first with the increase in amount dextran, then further increase in the amount of dextran causes increase in particle size. The size of nanoparticles were decreased with the increase in AA concentration but the excess AA was difficult to neutralize the reaction by 1 M NaOH, hence medium concentration of AA was selected that showed optimum size of nanoparticles. The optimized formulations was found to be (A3) for dextran and AA concentration (5:0.5), formulations (A3d) for stirring time (120 min.) and formulations (A3d4) for stirring speed (1600 rpm).

The nanoparticles was characterized for there size, shape, zeta potential and size distribution by Transmission Electron Spectroscopy (TEM) for size, Scanning Electron Microscopy (SEM) for shape, Zeta Nanosizer for Zeta potential and size distribution. The size of the plain and coated nanoparticles in TEM study was found to be of range 150-282 nm, and the average size of the nanoparticles was 207.67 nm (Figure 6). The % loading efficiency was a very important consideration to make the process economically acceptable. The optimum loading efficiency was found to be  $71 \pm 1.7\%$ .

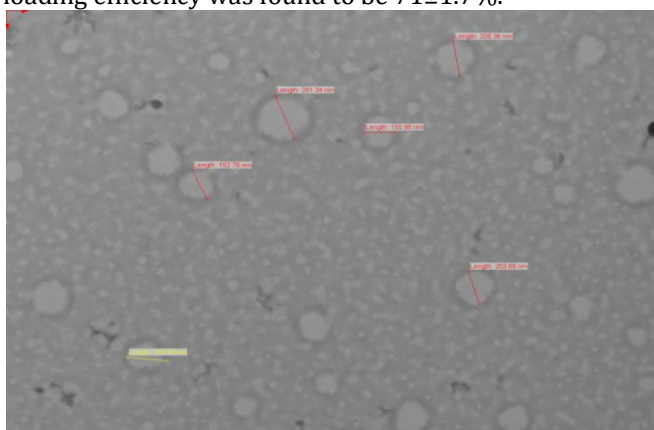


**Figure 6: Transmission Electron Microphotograph of Eudragit Coated Dextran Nanoparticles**

The average size of the nanoparticles was found to be 216 nm. The polydispersity index of the nanoparticles was 0.331 (count rate (kcps) was 169.4) (Table 6 and figure 7).

**Table 6: Zeta potential of Dextran Nanoparticles**

S. No.	Formulation	Zeta Potential	Particle size (nm)	P.D.I
1.	Dextran Nanoparticles	$-11.7 \pm 0.3$	$208 \pm 34$	0.331
2.	Eudragit coated dextran nanoparticles	$-14.1 \pm 0.2$	$267 \pm 30$	0.353

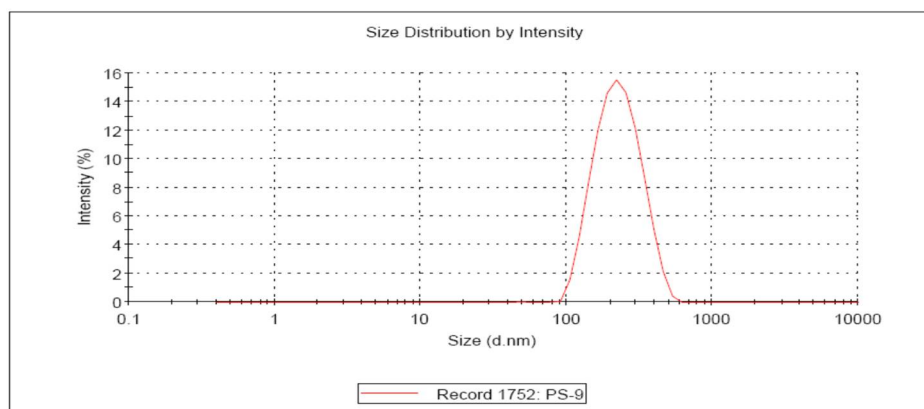


**Figure 7: Graph of size distribution by intensity**

The zeta potential of the final Nanoparticles formulation was found to be negative (Table 6 and Figure 8). The zeta potential value is an important particle characteristic as it can influence both particle stability as well as particle absorption. Zeta potential values, being positive or negative, tend to stabilize particle suspension. The electrostatic repulsion between particles with the same electric charge prevents the aggregation of the spheres. Absorption, on the other hand, can be promoted by a negative zeta potential value.

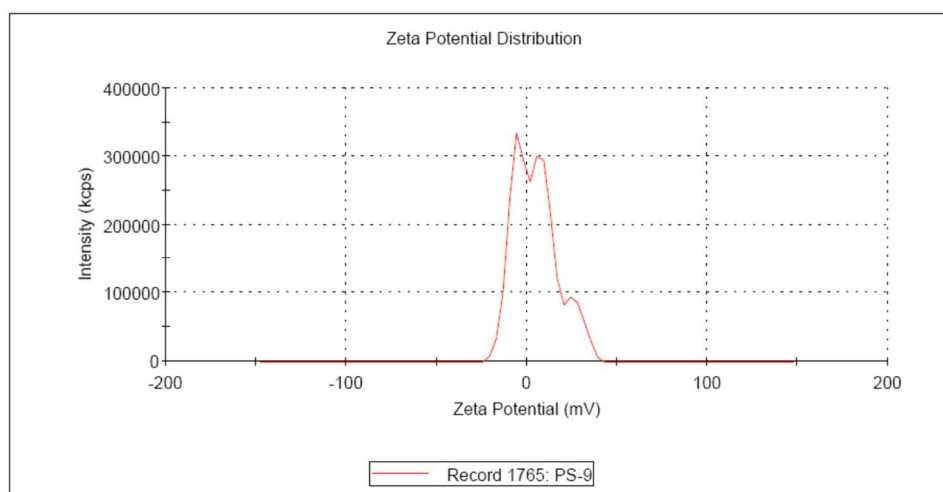


**Figure 8: Graph of zeta potential distribution**

In-vitro release profile was determined in PBS (pH 1.2 and pH 7.4) and shown in table 7 and presented in figure 9. A regular pattern of antigen release was monitored during 24hrs. The formulations showed continuous release in case of coated formulation at pH 7.4 and very poor release of antigen in case of pH 1.2. This showed coated formulation protects the antigen from acidic pH and release the antigen to the targeted M-cells of the intestine region. In-vitro release studies showed that around 20 % of the loaded protein was immediately released into PBS pH 7.4 which may be due to surface associated antigen release.

**Table 7: In vitro % Release**

Time (hrs)	% Release			
	pH 1.2		pH7.4	
	DNPs	ED.DNPs	DNPs	ED.DNPs
1	3±0.87	0.3±0.42	5±0.89	11±0.72
2	8±0.93	0.5±0.79	11±0.63	13±0.75
4	13±1.29	1±1.37	25±1.25	27±1.43
8	22±1.93	3±0.15	47±1.21	52±1.14
16	31±1.32	7±1.12	56±0.98	61±1.73
24	39±0.16	13±1.24	64±0.81	75±0.87

DNPs (dextran nanoparticles); ED.DNPs (Eudragit coated dextran nanoparticles)

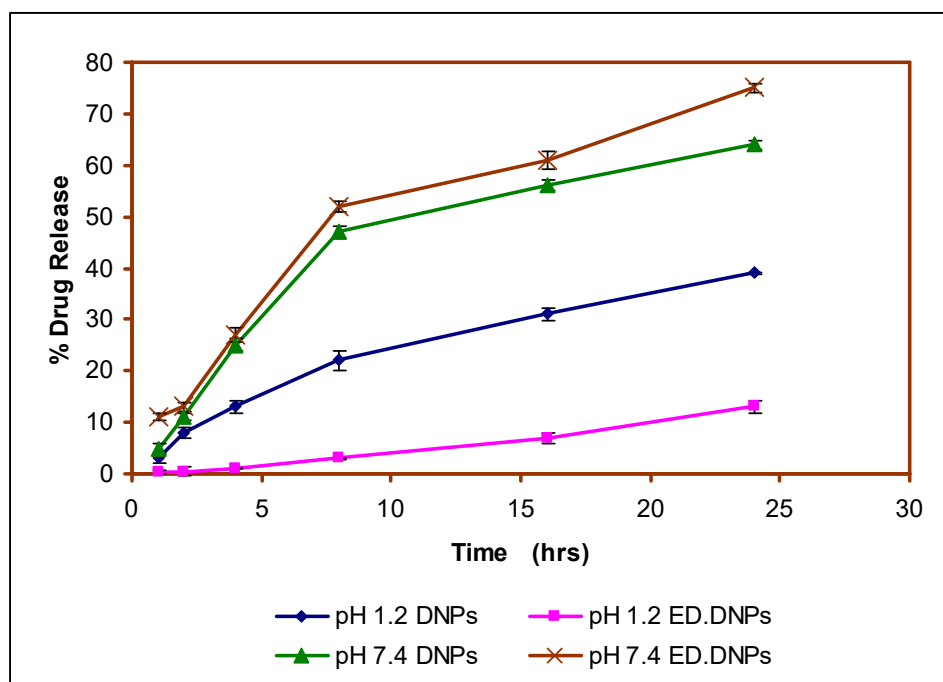


**Figure 9: Graph of In vitro % Release**

## CONCLUSION

In the research of new materials to obtain nanoparticles, we prepare a family of hydrophobically modified dextrans with the aim to use these materials for drug delivery applications. The solubility of modified dextrans in organic solvents depends on their HLB, i.e. on the substitution ratio and the hydrophobicity of grafted alkyl chains. Concerning the enzymatic degradation of chemically modified dextrans, the oral route could provide a suitable route for priming and boosting. Antigen for oral delivery can take many different forms including whole cells (virus, bacteria) surface proteins, synthetic peptide as well as DNA. Orally administration offers attractive alternative since it is possible to use smaller doses and to deliver the formulation to the appropriate site (GALT-Gut associated lymphoid tissue). In addition, because of the properties of the common intestinal immune system, the oral route can act as an inducer and effector site for the intestine, lungs and vagina. Hence, oral vaccines have an important role in the prophylaxis of Typhoid diseases.

## CONFLICT OF INTEREST

No conflict of interest

## ACKNOWLEDGEMENT

We would like to thank to School of pharmacy, SunRise University, Alwar for providing all facilities to conduct the research work.

## FUNDING RESOURCES:

None

## REFERENCES

1. Manukyan H, Wahid R, Ansari A, Tritama E, Macadam A, Konz J, et al. (2022). Quantitative RT-PCR assays for quantification of undesirable mutants in the novel type 2 oral Poliovirus vaccine. *Vaccines (Basel)* [Internet]. 10(9):1394. Available from: <http://dx.doi.org/10.3390/vaccines10091394>
2. Kowalska JD, Lara M, Hlebowicz M, Mularska E, Jabłonowska E, Siwak E, et al. (2023). Non-HIV-related comorbidities and uncontrolled HIV replication are independent factors increasing the odds of hospitalization due to COVID-19 among HIV-positive patients in Poland. *Infection* [Internet]. 51(2):379–87. Available from: <http://dx.doi.org/10.1007/s15010-022-01887-8>
3. Schlievert PM. (2023). Staphylococcal enterotoxin B and C mutants and vaccine toxoids. *Microbiol Spectr* [Internet]. e0444622. Available from: <http://dx.doi.org/10.1128/spectrum.04446-22>
4. Pandey SP, Bhaskar R, Han SS, Narayanan KB. (2023). Autoimmune responses and therapeutic interventions for systemic lupus erythematosus: a comprehensive review. *Endocr Metab Immune Disord Drug Targets* [Internet]. Available from: <http://dx.doi.org/10.2174/1871530323666230915112642>



5. Gaided H, (2017). In process control manager of diphtheria and tetanus plant, the holding company for the production of vaccines, sera and drugs (vacsera). Antiviral activity of secondary metabolites produced by *Streptomyces* species isolated from Egyptian soil. *Int J Adv Res (Indore)* [Internet]. 5(5):1165–74. Available from: <http://dx.doi.org/10.21474/ijar01/4227>
6. Tkachenko A, Özdemir S, Tollu G, Dizge N, Ocakoglu K, Prokopiuk V, et al. (2023). Antibacterial and antioxidant activity of gold and silver nanoparticles in dextran-polyacrylamide copolymers. *Biometals* [Internet]. Available from: <http://dx.doi.org/10.1007/s10534-023-00532-7>
7. Bradford EL, Gregory CL, Roman Longoria A, Jones KR, Bueren EK, Haak DC, et al.(2022). A new duplex qPCR assay for the quantification of honey bee (*Apis mellifera*) parasites *Nosema ceranae* and *Nosema apis* tested with low dose experimental exposure. *J Apic Res* [Internet]; 1–12. Available from: <http://dx.doi.org/10.1080/00218839.2022.2083846>
8. Blanco-Cabra N, Movellan J, Marradi M, Gracia R, Salvador C, Dupin D, et al. (2022). Neutralization of ionic interactions by dextran-based single-chain nanoparticles improves tobramycin diffusion into a mature biofilm. *NPJ Biofilms Microbiomes* [Internet]. ;8(1):52. Available from: <http://dx.doi.org/10.1038/s41522-022-00317-9>
9. Elmowafy M, Shalaby K, Elkomy MH, Alsaidan OA, Gomaa HAM, Hendawy OM, et al.(2023). Exploring the potential of quercetin/aspirin-loaded chitosan nanoparticles coated with Eudragit L100 in the treatment of induced-colorectal cancer in rats. *Drug Deliv Transl Res* [Internet]. 13(10):2568–88. Available from: <http://dx.doi.org/10.1007/s13346-023-01338-3>
10. Hosseini S, Wey K, Epple M. (2020). Enteric coating systems for the oral administration of bioactive calcium phosphate nanoparticles carrying nucleic acids into the colon. *ChemistrySelect* [Internet]. 5(31):9720–9. Available from: <http://dx.doi.org/10.1002/slct.202002846>
11. Solís-Cruz GY, Alvarez-Roman R, Rivas-Galindo VM, Galindo-Rodríguez SA, Silva-Mares DA, Marino-Martínez IA, et al. (2023). Formulation and optimization of polymeric nanoparticles loaded with riolozatrione: a promising nanoformulation with potential antiherpetic activity. *Acta Pharm* [Internet]. 73(3):457–73. Available from: <http://dx.doi.org/10.2478/acph-2023-0028>
12. Krishna SR, Ramu A, Vidyadhara S. (2020). Study of influence of formulation and process variables on entrapment efficiency and particle size of floating micro balloons of dipyridamole by doe. *Int J Pharm Pharm Sci* [Internet]. 85–91. Available from: <http://dx.doi.org/10.22159/ijpps.2020v12i10.35995>
13. Parashar AK, Patel P, Gupta AK, Jain NK, Kurmi BD. Synthesis, characterization and in vivo Evaluation of PEGylated PPI dendrimer for safe and prolonged delivery of insulin. *Drug Deliv Lett* [Internet]. 2019;9(3):248–63. Available from: <http://dx.doi.org/10.2174/2210303109666190401231920>
14. Parashar AK, Patel P, Kaurav M, Yadav K, Singh D, Gupta GD, et al. (2022). Nanomaterials as Diagnostic Tools and Drug Carriers. In: *Nanoparticles and Nanocarriers-Based Pharmaceutical Formulations*. Bentham Science Publishers; . p. 126–56.
15. Yadav P, Yadav AB. (2021). Preparation and characterization of BSA as a model protein loaded chitosan nanoparticles for the development of protein-/peptide-based drug delivery system. *Future J Pharm Sci* [Internet]. ;7(1). Available from: <http://dx.doi.org/10.1186/s43094-021-00345-w>
16. Parashar AK. (2021). Synthesis and characterization of temozolomide loaded theranostic quantum dots for the treatment of brain glioma. *J Med Pharm Allied Sci* [Internet]. 10(3):2778–82. Available from: <http://dx.doi.org/10.22270/jmpas.v10i3.1073>

#### CITATION OF THIS ARTICLE

Ramakant P, Vishal Bharat B- Preparation, Optimization and Characterization of Recombinant Typhoid (Ty21a) Antigen Encapsulated Eudragit Coated Dextran Nanoparticles. *Bull. Env. Pharmacol. Life Sci.*, Vol 12[11] October 2023: 48-56